Inkjet Printing for Advanced Semiconductor Packaging:
Pillars and Through-silicon Vias (TSVs)

Jacob Sadie, Vivek Subramanian

Department of Electrical Engineering and Computer Sciences
University of California, Berkeley

“Smaller, faster, lighter, cheaper…”

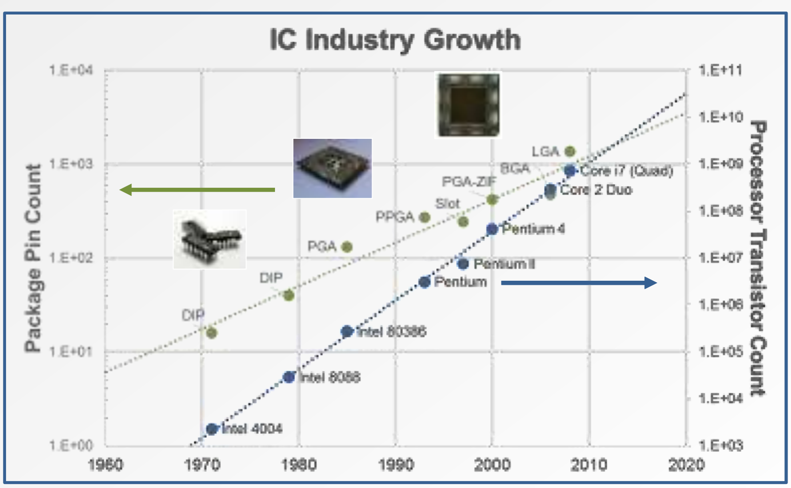

CMOS scaling drives the need for denser, higher performance, and higher reliability packaging

The Future of BEOL Packaging

Next Generation Packaging Approaches

FUNDAMENTAL PACKAGE PERFORMANCE METRICS:

- **Pin Density**
- **Pin Count**
- **Transistor Density**

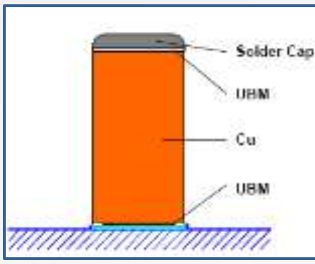

Copper post and solder cap

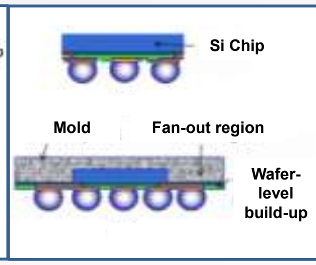

Fan-in and fan-out design

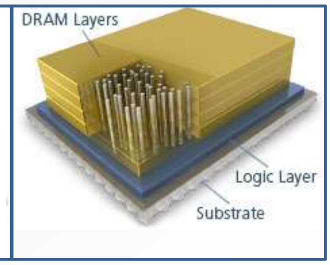

Through-silicon vias (TSVs)

Novel approaches are needed to meet demands of new applications that require higher density and thinner packages.

Conventional Post Processes

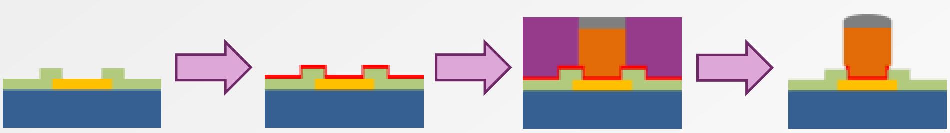

Passivation / Under Bump Metallization / Cu Electroplating / Solder Reflow

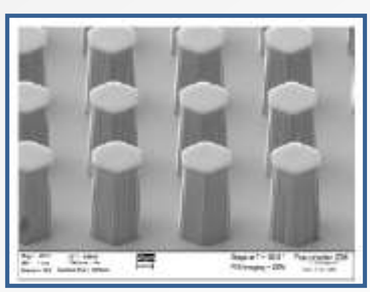

Complex Process
Prone to Intermetallics
Pb-free solders still problematic

4

Conventional TSV Processes

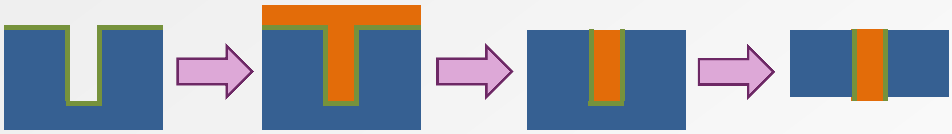

Liner Deposition / Cu Electroplating / CMP / Wafer Thinning

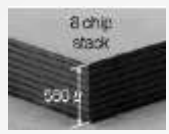

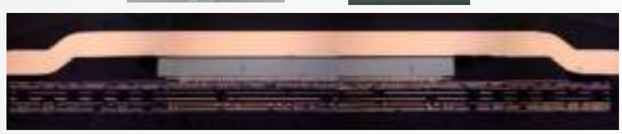

Pattern-sensitive
Expensive
Keyholes and Stress Concerns
Difficult Scaling

5

Inkjet-Printed Electronics

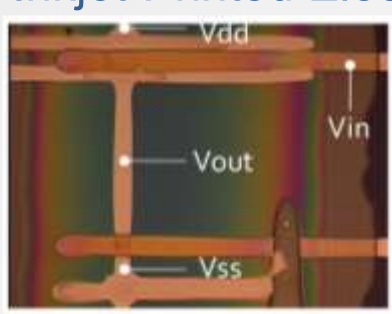

Self-aligned Inverters

MEMS Switches

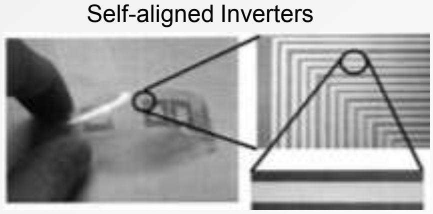

Metal Nanoparticle Inks

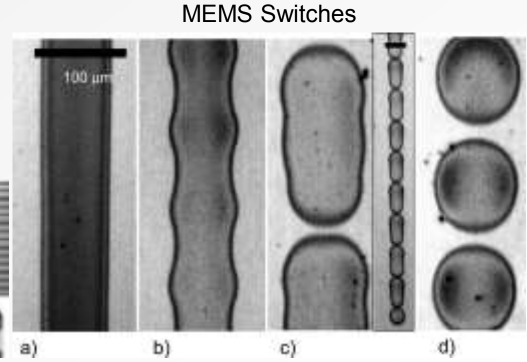

Highly-controlled Line Morphology

6

Research-Grade Inkjet Printing

MicroFab Single Nozzle

Fuji Dimatix 16 Nozzle

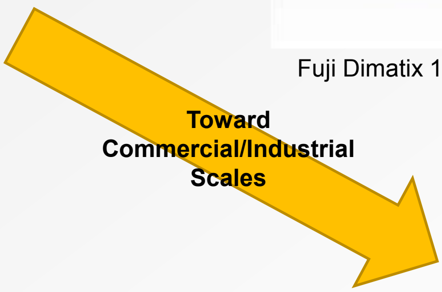

Fuji Dimatix 128 Nozzles

7

Inkjet Printing for Packaging Applications

- ✓ Additive
- ✓ Adjustable-on-the-fly
- ✓ Vacuum-independent
- ✓ Mask-independent
- ✓ Scalable
- ✓ Diverse material set
- ✓ New substrate technologies

- Inkjet critical dimension *smaller* than projected packaging scaling trends

Inkjet printing positioned as a viable long-term solution for packaging materials deposition, but materials and processes still require development

8

Nanoparticles as Interconnect Materials

Nanoparticle Sintering Process

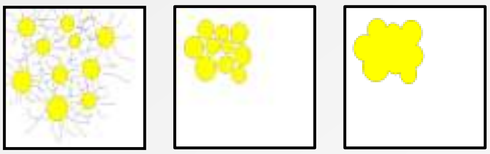

Encapsulated nanoparticles dispersed in ink | Encapsulant bonds break; nanoparticles coalesce | Nanoparticles neck and form film

Apply Heat

Gold Melting Point Reduction

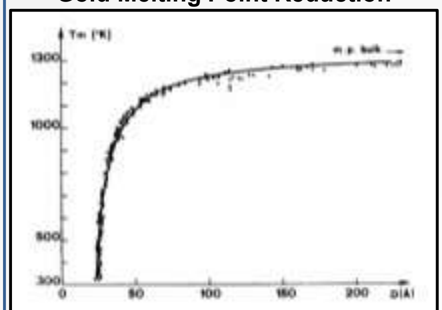

Gold melting point can drop to below 200 °C

Nanoparticle inks offer compatible processing temperatures, improved material and substrate selection, and reduced cost for interconnects

1. Kubelka-Prag, Zuchr. Elektrochem., 38 (8a), pp. 611-614 (1932)
2. Buffat and Borel, Phys. Rev. A, 13 (6), pp. 2287-2298 (1975)
3. Huang *et al.*, J. Electrochem. Soc.,150 (7), pp. G412-G417 (2003)

The Challenges:

How can we inkjet-print metal nanoparticle inks in three dimensions?

How does sintering alter the material properties of these structures?

How do these structures compare to conventional materials/processes?

Pillars

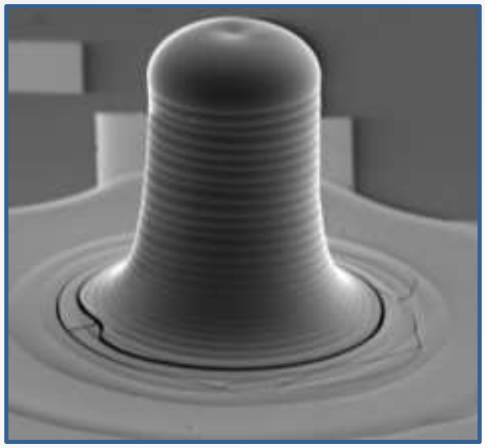

3D Printing Technique

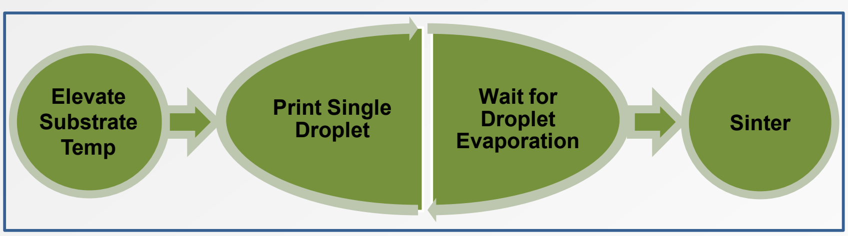

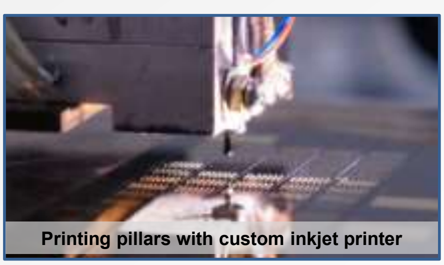

Printing pillars with custom inkjet printer

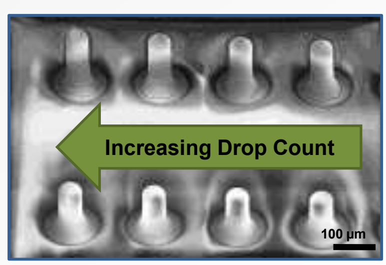

Using a drop-wise printing on heated substrates, we are able to fabricate free-standing pillars. Drop frequency and substrate temperature are primary controls.

12

High Aspect Ratio Pillars

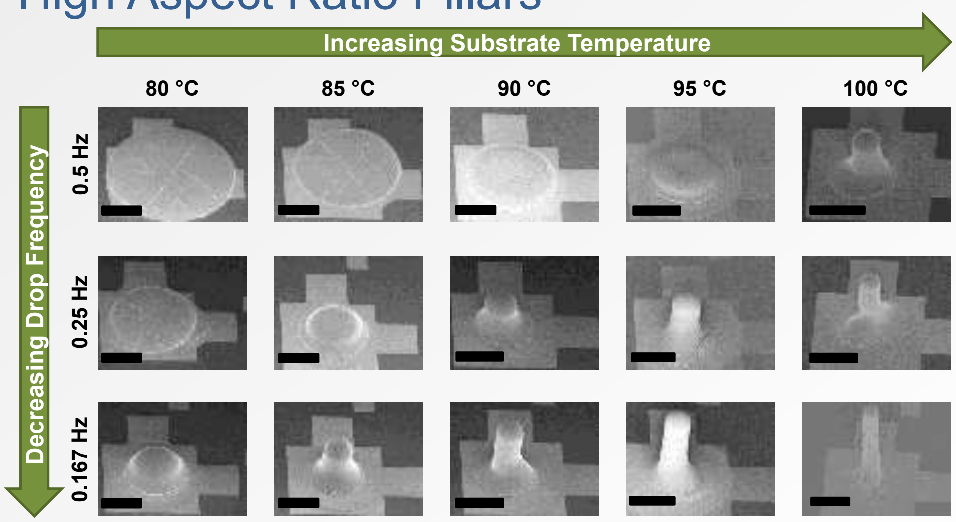

Experimental Details:
Ink: **Harima NPG-J gold nanoparticle ink**
Substrate: **Evaporated Cr/Au pads on SiO_2**
Total drops per pillar: **50**

Images: **SEM, all scale bars are 100 µm**

13

High Aspect Ratio Pillars

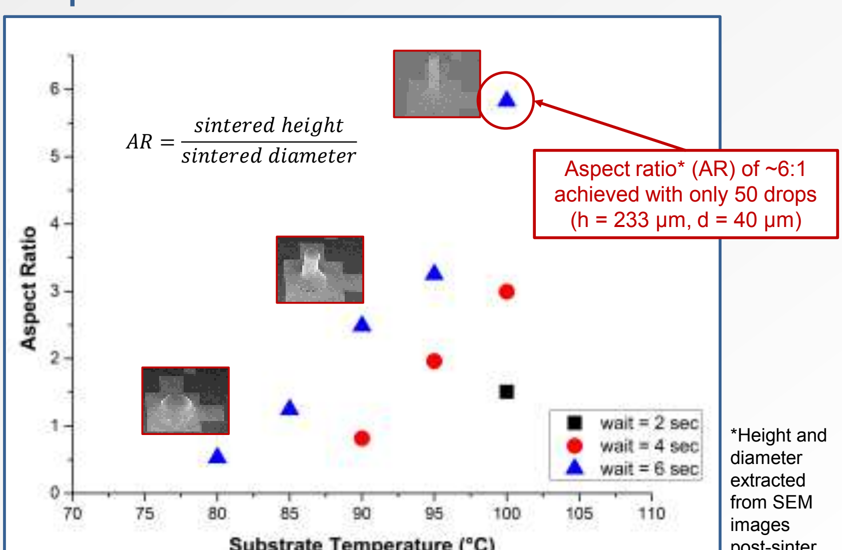

*Height and diameter extracted from SEM images post-sinter

Adjusting substrate temperature and jetting frequency allows us to achieve pillars with very high-aspect ratios

14

Material Properties of Importance

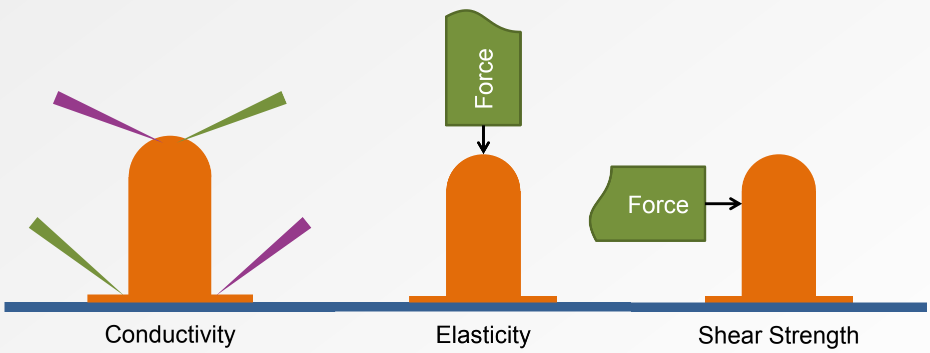

In these relatively large nanoparticle-based structures, how does sintering proceed/determine the ultimate material properties?

Pillar Resistance Model

Thin-film nanoparticle inks commonly use resistance as metric to indicate degree of sintering.

How do we do the same for our pillars?

Resistance Model:

1. Pillar is perfect cylinder

$$R_{pillar} = \frac{\rho_{pillar} h}{\pi r^2}$$

2. After taper regime:

$$h \propto drops$$

$$R_{pillar} \propto h \rightarrow R_{pillar} \propto drops$$

3. Resistivity a function of sinter condition:

$$\rho_{pillar} \rightarrow \rho_{pillar}(t, T)$$

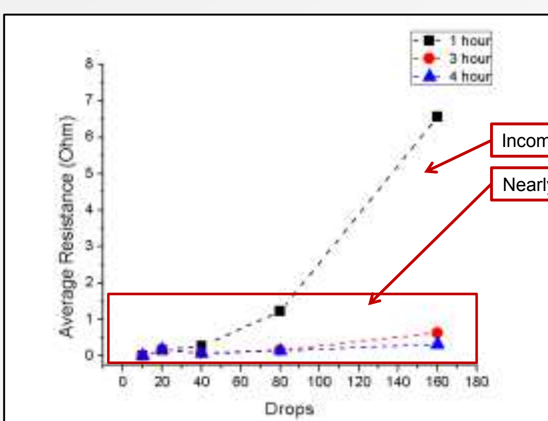

When sintering complete, resistivity should be constant as drop number increases and resistance should be proportional to drop count

16

Pillar Resistance Model

Thin-film nanoparticle inks commonly use resistance as metric to indicate degree of sintering.

How do we do the same for our pillars?

Resistance Model:

1. Pillar is perfect cylinder

$$R_{pillar} = \frac{\rho_{pillar} h}{\pi r^2}$$

2. After taper regime:

$$h \propto drops$$

$$R_{pillar} \propto h \rightarrow R_{pillar} \propto drops$$

3. Resistivity a function of sinter condition:

$$\rho_{pillar} \rightarrow \rho_{pillar}(t, T)$$

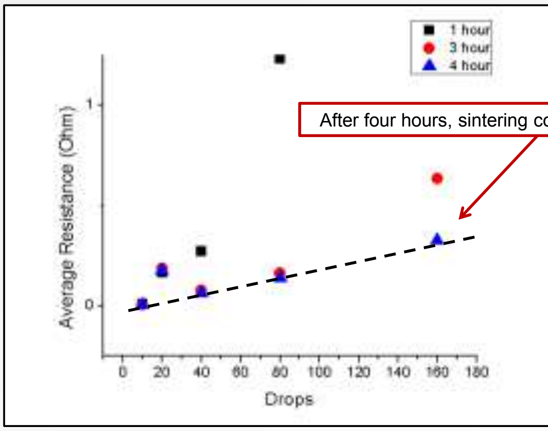

When sintering complete, resistivity should be constant as drop number increases and resistance should be proportional to drop count and we can extract effective resistivity value

17

Pillar Resistance as a Function of Sintering

A 140°C sinter condition and short sinter times resulted in immeasurably high resistance

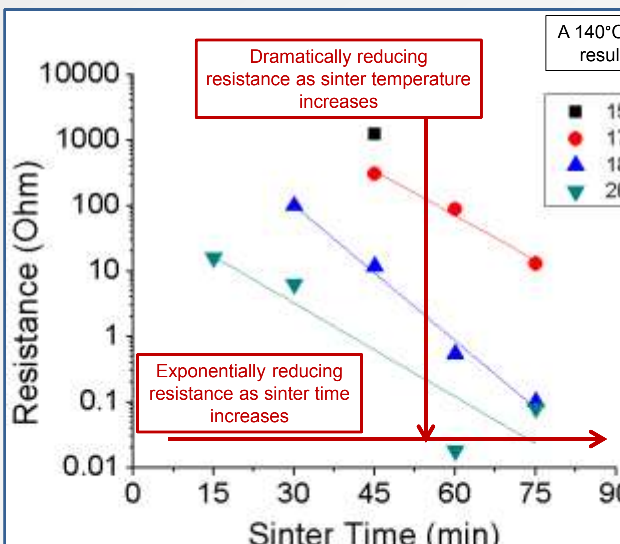

Experimental Details:
Ink: **Harima NPG-J gold**
Substrate temp: **100 °C**
Time between drops: **4 sec**
Total drops per pillar: **30**

Material	Conductivity (S/cm)
Bulk Gold	4.54E05
Harima Gold (thin film)	1.43E05
Tin Silver Copper	7.69E04
Harima Gold (pillars)	**7.58E04**
Lead Tin Eutectic	6.94E04
Gold Tin	6.10E04

Highest extracted conductivity outperforms conventional eutectic solder but still requires higher thermal treatment

18

Nanoindentation

Solder bump loading capacity a critical parameter to extract

Extracted elasticity with nanoindentation at LBNL

$$E_r \propto S \propto \frac{\mathrm{d}}{\mathrm{d}d} L(d)$$

Load-Displacement Curves

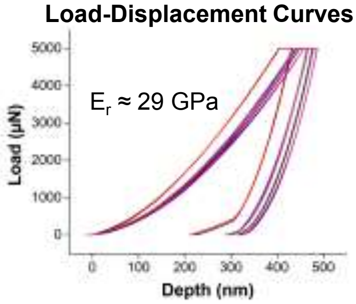

*Sample curves sintered at 200 °C for 75 min and loaded at 200 μN/s

Nanoindentation Test Schematic

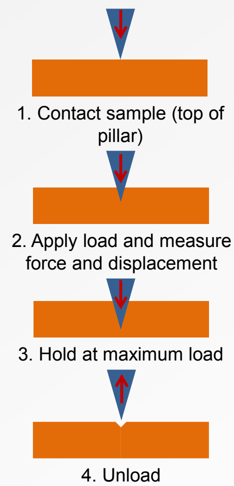

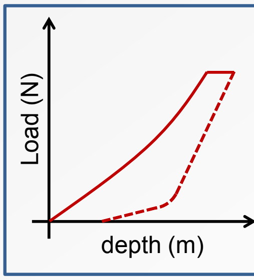

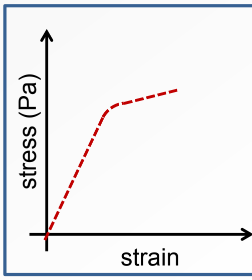

Pillar Elasticity as a Function of Sintering

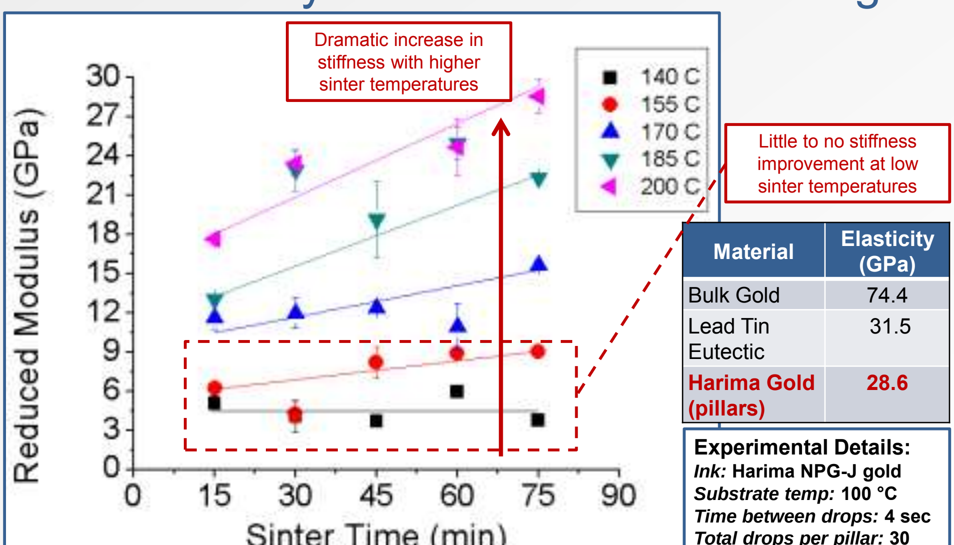

Material	Elasticity (GPa)
Bulk Gold	74.4
Lead Tin Eutectic	31.5
Harima Gold (pillars)	**28.6**

Experimental Details:
Ink: **Harima NPG-J gold**
Substrate temp: **100 °C**
Time between drops: **4 sec**
Total drops per pillar: **30**

Highest extracted modulus (29 GPa) comparable to conventional eutectic solders

Pillar Shear Strength

- Printed arrays of pillars (nominally 20 pillars per array)
- Oven-sintered each array for one hour
- Performed shear testing with Dage 4000 at 100 µm/s shear rate
- SEM images used to characterize failure mechanisms

- **Observed Failure Mechanisms:**
  - **Interfacial failure**
  - **Sloped Ductile failure**
  - **Flat Ductile failure**

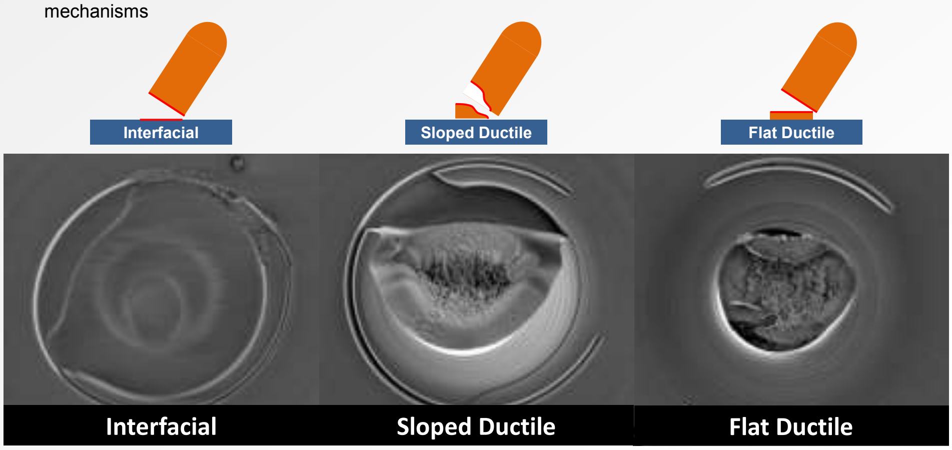

Shear Strength and Failure Rates

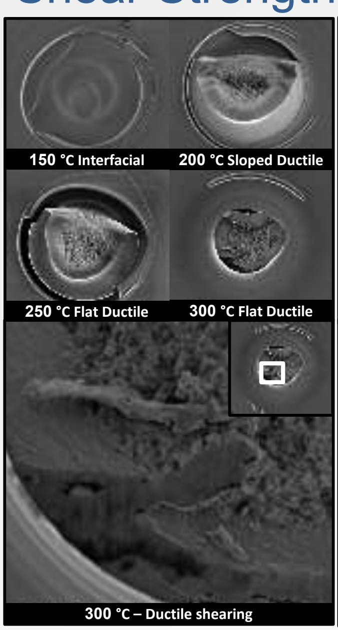

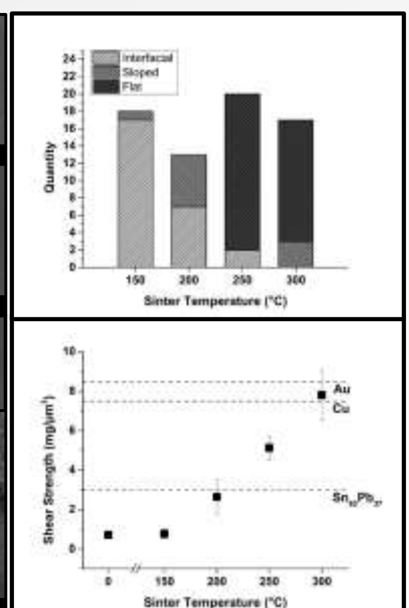

Key Results:

Interfacial failures dominant at low sinter temperatures

Ductile shearing dominant at higher sinter temperatures and two failure modes observed:
→ 'Sloped' at lower temperatures

→ 'Flat' at higher temperatures

Absolute shear strength competitive with lead-tin eutectics and bulk gold at 200 C and 300 C, respectively

Pillar Compaction

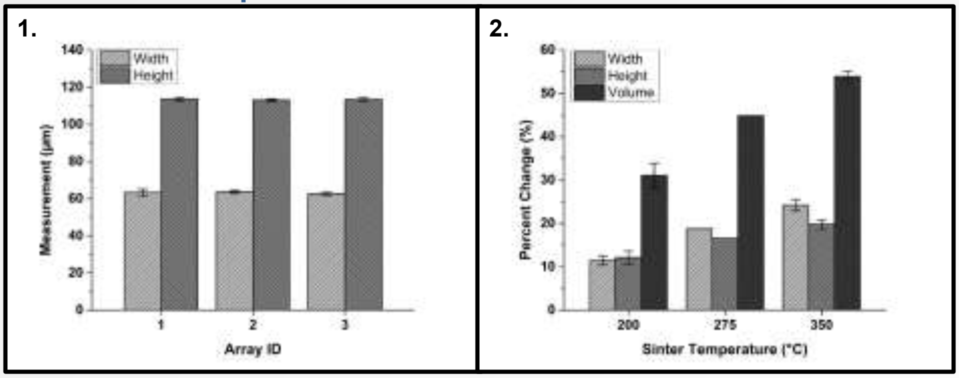

Using confocal 3D microscope, measured pillar height and width as a function of sintering conditions

Key Results:
Highly uniform printing (fig 1) with height and width tolerances within 1.5 μm each
Pillars exhibit both lateral AND vertical compaction
Extracted volume compaction of 53% in highest sintering condition
Compaction primarily driven by substrate temperature as opposed to sinter time

Properties ⇔ Structure/Composition

- All observed dynamic properties must correlate to change in structure or composition of printed features
- During sintering, de-encapsulation and outdiffusion of nanoparticle encapsulant will cause shifts in electrical and mechanical response of pillars
- Ideal situation is complete removal of all carbon-based encapsulant, but highly likely carbon becomes trapped inside structures
- Tests to investigate these questions include focused ion beam (FIB) and energy-dispersive x-ray spectroscopy (EDX)

FIB Milling of Sintered Pillars

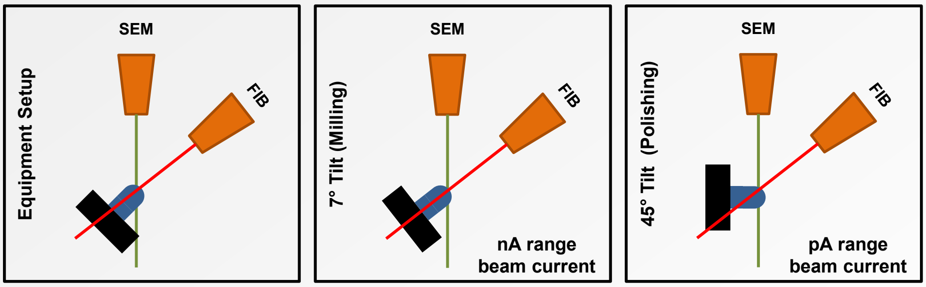

FIB Milling and Sample Preparation:

1. Sample placed on 45° and placed into tool
2. Sample tilted 7° to align axis along FIB beam for milling down center of pillar (beam current in nA range)
3. Sample tilted 45° to polish small section of milled pillar to prepare for EDX scans (beam current in pA range)

FIB Milling of Sintered Pillars

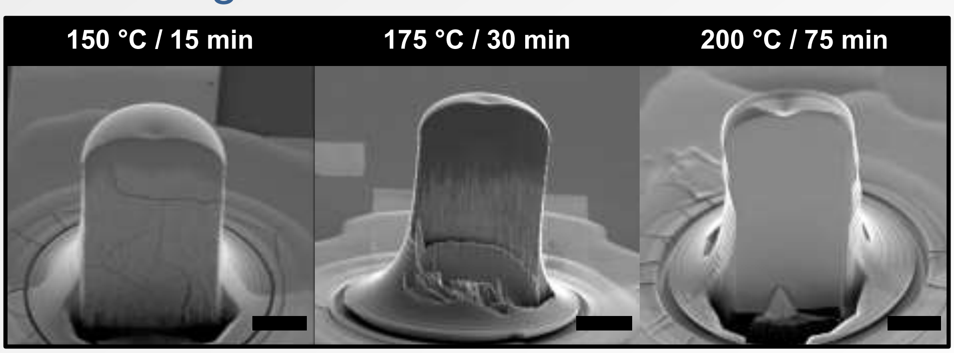

FIB of pillars sintered to varying degrees result in extremely varied milled surfaces:

Waterfall effect: Effect whereby milled surfaces exhibit a curtain-like appearance; often attributed to highly disparate atomic masses in material composition (e.g. C and Au)

- Observed in 150 C and 175 C condition but not 200 C condition
  → Evidence of waterfall effect is qualitative measure of quantity of residual carbon content in pillars

Cracking:

- Cracks seen in mildest sintering condition only

EDX Scans of Polished Pillars

- Require smooth surfaces to more confidently assess material composition
  → Only able to perform reliable scans on 200 C sintered structures (after 10 pA polishing prep)
- **Results:**
  - **Compare C and Au peaks throughout pillar**
  - **In base and center scans (a.-c.), Au is predominant element observed, with C signal roughly half of Au signal**
  - **At top of pillar (d-e), C and Au signals comparable and C primarily located at center of pillar**

Sintering front moving from bottom to top of pillar and carbon at center has potential to remain trapped in structure (longer path for outdiffusion)

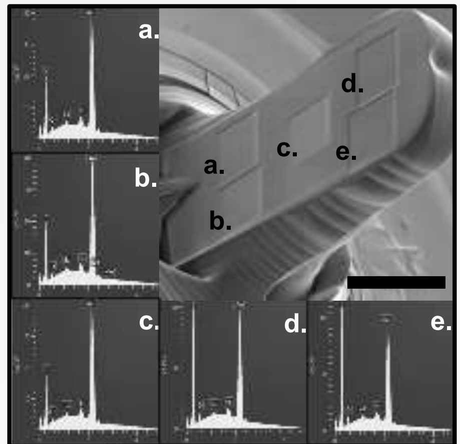

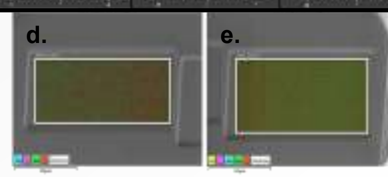

Putting it All Together: A Cross-Sectional View of Sintering Front

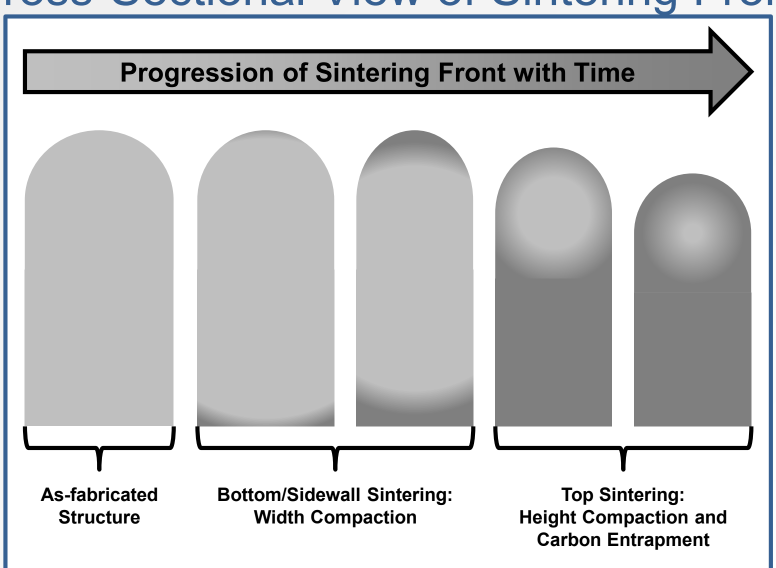

Pillar Review

- Uniform/reliable 3D-printing process of functional inks
- High conductivity pillar structures at sinter temperatures not to exceed 200 °C
- Elastic modulus comparable to conventional eutectics
- Shear strength comparable to conventional eutectics at eutectic process temperatures and comparable to bulk properties at 300 °C

Through-silicon Vias (TSVs)

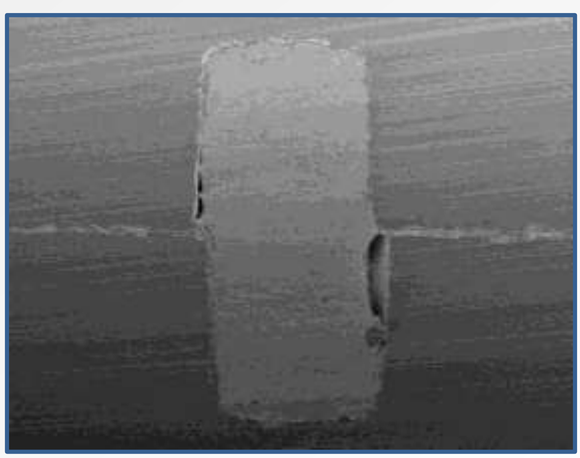

Inkjet-Printed TSVs: Fill and Bump

Leverage existing solder bump process to establish TSV nanoparticle process

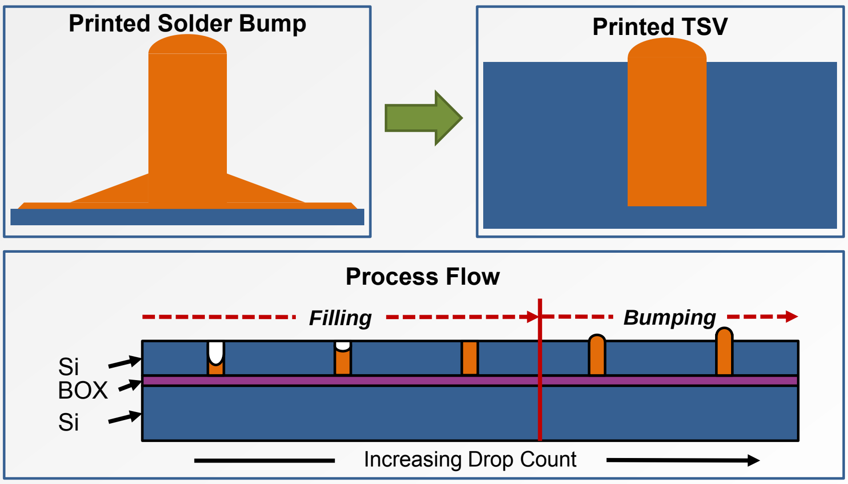

The ability to both fill AND bump in the same process is a highly impactful and unique capability of inkjet-printed TSVs

31

Fully-tunable TSV Fill and Bump

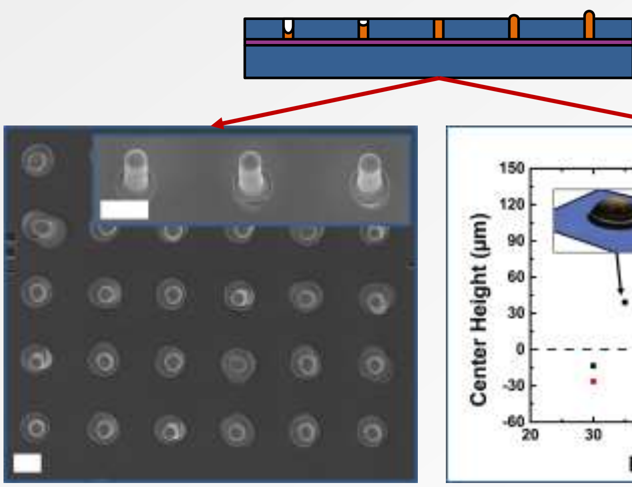

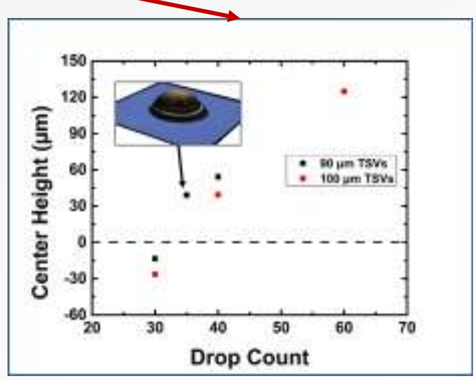

Scale Bars: 100 μm

Substrate Temperature: 120 °C
Drop Delay: 8 sec

Complete arrays of filled and bumped TSVs fabricated by tuning the printing parameters: substrate temperature, drop delay, and total drop count

32

Keyhole-free Via Fill and Bump

Top-Down SEM

At a given temperature and wait time, varying drop number leads to pillar growth out of a TSV

80 μm diameter vias
140 °C
7 sec wait

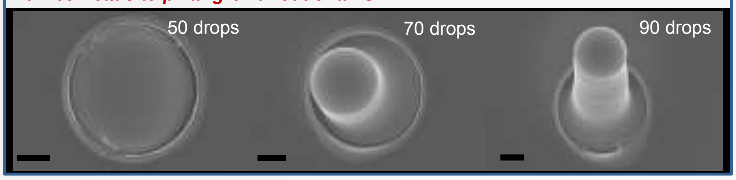

Cross-section SEM

Cross-sectional analysis shows keyhole-free filling of TSVs throughout filling/pillar growth regimes

80 μm diameter vias
140 °C
7 sec wait

*All scale bars represent 20 μm
*All TSVs sintered at 200 °C for 60 min

33

TSV Bonding Schemes and Test Structures

Bonding Schemes

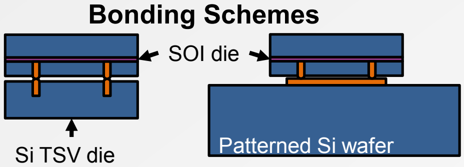

1. Die-to-die **2. Die-to-wafer**

Test Structure Fabrication Process

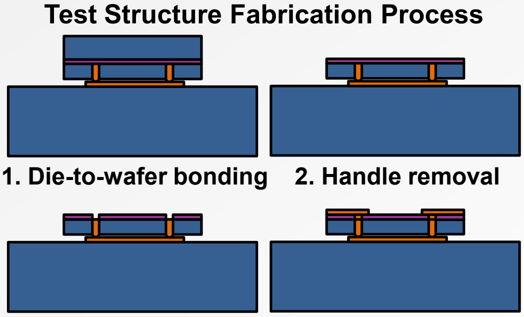

1. Die-to-wafer bonding **2. Handle removal**

3. Oxide patterning **4. Top metal patterning**

Mechanical Test Structure

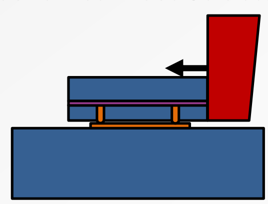

Electrical Test Structure

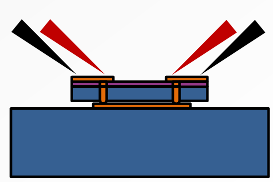

34

Via Bonding and Reflow

Bonded TSVs

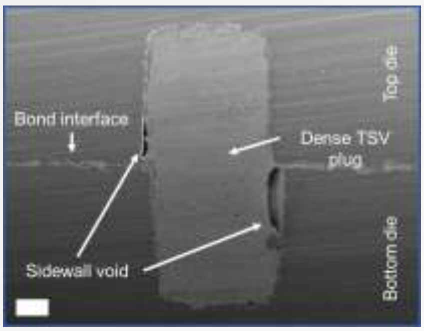

Cross-sectional SEM image of die-to-die TSV bonds (20 μm scale bar)

Reflow

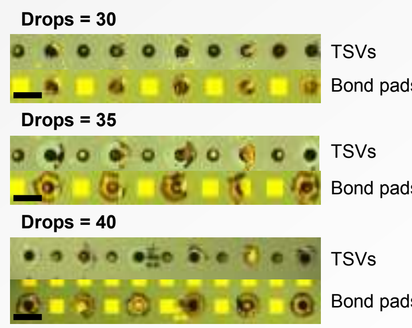

Bonded die sheared to observe extent of reflow (250 μm scale bar)

Cross-sectional analysis reveals dense filling of TSV and post-shear testing indicates reflow-like behavior of nanoparticle bumps

35

Electrical and Mechanical Performance

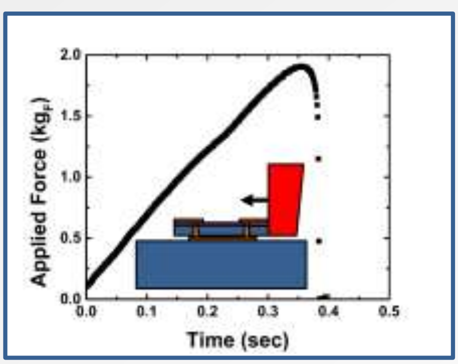

Maximum die shear strength = 1.9 kg_F for die bonded with 144 TSVs

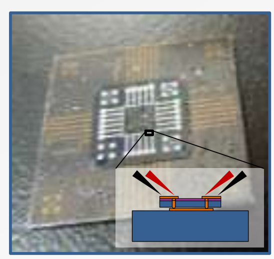

Sample bonded and prepared for electrical testing

	Extracted Resistance (Ω)	Conductivity (S/cm)
TSV	3.5E-02	**3.34E03**
Pillar	1.2E-02	**7.58E04**
Bulk Gold	N/A	**4.54E05**

Extracted resistance less than 1 Ω, but conductivity still much lower than printed pillars and bulk gold

Metal nanoparticle-based inkjet-printed TSVs show much promise for future TSV filling and bumping applications.

36

TSV Review

- Successfully transitioned solder bump inkjet processes to TSV filling and bumping process
- Demonstrated complete process flow for flip-chip bonded TSV die including reflow-like behavior during bond
- TSV mechanical and electrical properties show much initial promise. Plenty of room to improve performance with optimized sintering and bonding processes.

37

Acknowledgements

- Ultratech, Inc.
- DARPA
- Berkeley Sensor and Actuator Center (BSAC)
- The Printed Electronics Group at Berkeley
- Marvell Nanolab

38